

CARBON DOPED TiO₂ THIN FILMS FOR PHOTO CATALYTIC APPLICATIONS

N.M.GANESAN^{a*}, N.MUTHUKUMARASAMY^b,
R.BALASUNDARAPRABHU^c, T.S.SENTHIL^a

^a*Department of Physics, Erode Sengunthar Engineering College, Erode*

^b*Department of Physics, Coimbatore Institute of Technology, Coimbatore*

^c*Department of Physics, P.S.G.College of Technology, Coimbatore*

Nanocrystalline TiO₂ is a highly suitable material for photo catalytic applications. TiO₂ nanocrystals have been synthesized by simple sol-gel method at different pH values. By using liquid impregnation method carbon doped TiO₂ nanocrystal has been prepared. Carbon doped TiO₂ nanocrystalline thin films have been prepared by doctor blade method. The photo catalytic activities of the prepared carbon doped TiO₂ nanocrystalline thin films are investigated based on oxidation and decomposition of methylene blue in aqueous solution. The photo catalytic study has been carried out using UV visible spectrometer. It has been confirmed that the pH of the sol plays a vital role in photo catalytic application. TiO₂ nanocrystals synthesized using pH = 10.6 shows considerable degradation of methylene blue than the nanocrystals synthesized using other pH values.

(Received April 28, 2013; Accepted October 2, 2014)

Keywords: TiO₂ nano crystals, Sol – gel method, pH value, Liquid impregnation method

1. Introduction

Titanium dioxide is one of the widely used photo catalytic material because of its high specific surface area, chemical & physical stability, outstanding photocatalytic activity and stability towards photo corrosion [1,2]. Because of its strong oxidizing power of photo-generated holes, chemical inertness, and nontoxicity, TiO₂ photocatalysis offers promising technologies for chemical synthesis, environmental purification, energy renewal, and energy storage [3]. Unfortunately, because of its wide band gap (3.2 eV) it can be activated only under UV light irradiation. However it is reported that the nanocrystalline TiO₂ can absorb about 5% of the sunlight from UV region. It will have a positive effect for improving the photocatalytic efficiency of TiO₂ by shifting its optical response to the visible range. To increase the absorption rate of visible light by narrowing the band gap energy and lower the e-h recombination, there are several attempts have been made [4]. Among them doping some transition metal is important but these metal-doped photocatalysts have been shown to suffer from thermal instability, and metal centers act as electron traps, which reduce the photocatalytic efficiency [5-8]. Recently, doping TiO₂ with nonmetal atoms such as nitrogen [9, 10], carbon [2, 6, 8, 11, 12], and sulfur [13] has received much attention. Because nonmetals may be more appropriate for the extension of photocatalytic activity of TiO₂ into the visible-light region because impurity states are near to the valence band edge, but do not act as charge carriers. Furthermore, their role as recombination centres might be minimized as compared to metal doping. Although doping with nitrogen and sulfur shows a similar band gap narrowing [14], it would be difficult to incorporate it into the TiO₂ crystal because of its large ionic radius [9]. Doping with carbon results in about a 50 nm red shift in the absorption spectra [9,12,14], and improved photoactivity in the visible-light region by decreasing the recombination rate in photogenerated electron-hole pair with doped carbon as electron scavengers. The photo catalytic activity is also determined by its crystalline phase of TiO₂ [15]. The hydrolysis condition has an influence on the phase composition. It has also been reported that specific morphology can be obtained by changing the hydrolysis media [16]. Even though the TiO₂ nanocrystal provides high catalytic surface area and photo catalytic activity but after the application it is difficult to remove it from the suspension [17]. This problem can be overcome by using TiO₂ in thin film form. Activity of immobilized catalyst is very low and to increase the absorbance ability of the immobilized photo catalyst, carbon can be used [18]. To synthesis TiO₂

* Corresponding author: nmgsec@yahoo.com

nanocrystals there are variety of methods have been used such as sol-gel, hydrothermal, and co-precipitation method [19-21]. Out of the different methods available for the preparation of TiO₂ nanoparticles, the sol-gel method is simple, inexpensive, non-vacuum and low temperature technique [19]. In the present work sol gel method is used to synthesize TiO₂ nanocrystals and carbon doping is done using liquid impregnation method. The carbon doped TiO₂ thin film is formed by using doctor blade method. In this study, the morphology, and optical properties of the as-prepared nanomaterials were investigated systematically using various characterization tools. The photocatalytic activity was evaluated for degradation of methylene blue under visible light irradiation.

2. Experimental

Titanium isopropoxide (Alfa Aaser 99.9%) has been used as the titania precursor. Absolute ethanol (Hayman 99.9%) has been used as a solvent. The desired pH (pH=2.6, 7, and 10.6) of the sol was controlled by adding dilute nitric acid and sodium hydroxide. Titanium isopropoxide is added drop wise to ethanol with stirring. After one hour stirring, nitric acid /sodium hydroxide is added to achieve the desired pH. The final sol is dehydrated in open atmosphere at 70°C for the desired period of 48 h for the nucleation and growth of TiO₂ nanoparticles. The resulting nanoparticles were washed with distilled water and the obtained solution was centrifuged at 5,000 rpm for 10 min, the washing and centrifuging was repeated several times in order to remove the impurities completely from the nanoparticles, and then the sample was dried at 70°C for 1 h. The synthesized nanoparticles were annealed at 425°C for 30 min.

Azadirachta indica, also known as Neem leaves were used to prepare Carbon, collected Neem leaves were cleaned and washed and sun dried for 24hrs. The samples were crushed in order to be processed further in the furnace. Carbonization of the precursor was carried out at a temperature of 500°C, the carbonization was achieved in a muffle furnace for 4hrs. The prepared carbon was further treated by HCl (0.1M) and NaOH (1M) and Ammonia solution. Then the moist activated carbon was kept in the furnace at 550°C (activated temperature) to increase the porosity of the activated carbon. The resulting activated carbon was washed with distilled water and dried in the furnace at 100°C for 2hrs. It was then packed in the dry container. Using liquid impregnation method Carbon-doped TiO₂ (C-TiO₂) nanoparticle was synthesized according to the following steps. First, 2 g of synthesized TiO₂ nanocrystals was added to 50 ml deionized water. Then the required amount of prepared carbon was added to TiO₂ suspension, the slurry was stirred well. The mixed solution was then transferred into a 100ml Teflon autoclave without stirrer, sealed with a stainless steel lid, and aged at 160°C for desired period of 24h for the nucleation and growth of carbon doped titania particles. After the end of the reaction, the mixture was cooled in a natural way. The obtained solid products were centrifuged and washed with distilled water, followed by drying at 80°C in air.

To prepare C-TiO₂ thin films, the paste was prepared as described by Chae et al., [22]. Briefly, paste was produced by mixing 2.0 g of C-TiO₂ powders with a mixture consisting of 5.0 g of α -terpineol, 0.5 g of cellulose, and 20 ml of ethanol, which was sonicated for 24 h at 1,200 Wcm⁻². By using the prepared paste C-TiO₂ thin films were prepared by coating the paste on a well cleaned glass substrate using doctor blade technique. The prepared films were annealed at 425°C for 30 min. To identify the crystal structure, X-ray diffraction studies were carried out using Shimadzu (Model - XRD 6000), X-ray diffractometer with nickel-filtered CuK α (30 kV, 30 mA). The surface morphology of the samples was studied using scanning electron microscopy (SEM; JSM6390, JEOL). The absorbance spectra have been recorded using a spectrophotometer JASCO V-570. Photo catalytic activity was carried out in a specially designed reactor in which the light source was 8W UV lamp (Philips TUV-08). The prepared C-TiO₂ thin films were used as catalyst. 0.5 mol of methelene blue dye was taken in a beaker and C-TiO₂ thin films were suspended into the beaker and treated with UV lamp by varying irradiation time and pH of the nanocrystals. The absorption spectra were recorded using UV-Vis spectrophotometer and rate of decolorization was observed.

3. Results and Discussion

The X-ray diffraction pattern of C-TiO₂ nanocrystals annealed at 425°C and prepared using different pH conditions (pH=2.6, 7, and 10.6) are shown in Fig. 1. The C-TiO₂ nanocrystals prepared at pH=2.6 shows the peaks at 2 θ values of 25.14, 27.30, 37.67, 47.89, 53.80, 54.92, 62.44

and 68.7. These 2θ values correspond to (101), (102), (004), (200), (105), (211), (213), and (116) planes of anatase phase of TiO_2 and are in good agreement with standard JCPDS data (82-2243). The typical peaks in diffraction pattern for the C- TiO_2 nanocrystals synthesized using pH= 7 and pH= 10.6 are also shows the planes of anatase phase. From these results it is seen that only the anatase phase is present in all the samples. The dominance of anatase phase is considered as a favorable condition for the enhancement of photo catalytic activity in TiO_2 . The average grain size estimated by using Scherrer's equation for the (101) peak. The calculated grain size and the lattice parameter values a and c are tabulated and it is shown in Table 1. It is observed that the particle size increases with increase of pH. However the d spacing is more or less same. This implies that the doping process does not change the average unit cell dimension. The growth of the particle size is due to the result of the charges present on the surface of TiO_2 nano crystal in lower pH and higher pH conditions, both pH conditions can restrain the crystallization speed by Coulomb force [23].

Table.1 Particle size and structural properties of C- TiO_2 nanocrystals

pH Values	Particle size (nm)	a – value (nm)	c- value (nm)	d-spacing (nm)
2.6	19.7	3.81	10.07	3.53
7.0	21.2	3.20	10.05	3.56
10.6	22.6	3.80	10.04	3.55

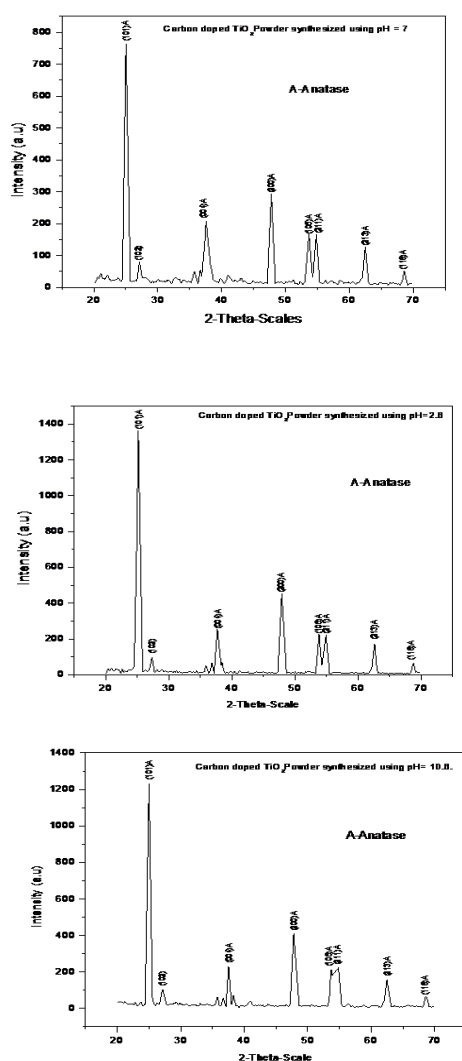


Fig. 1. X-ray diffraction pattern of C- TiO_2 nanocrystals prepared using different pH values

Fig. 2 (a,b and c) shows the SEM images of C-TiO₂ nanocrystals prepared at different pH values. The SEM images show the presence of carbon particles on the agglomerated TiO₂ nanocrystals. The shape of the TiO₂ nanocrystals synthesized at all pH values appears like a rectangular slab. It has been observed that the size of the carbon particles and TiO₂ nanocrystals increases with increase of pH values. Figure 2 (d) shows the EDXA pattern of C-TiO₂ nanocrystals and the compositional analysis shows the presence of Ti, C and O. The TEM image of C-TiO₂ nanocrystal prepared at pH=10.6 is shown in Figure 3 (a) and (b). The figure clearly shows that the particle size is found to be in the range of ~20 nm and it is in good agreement with the particle size calculated from XRD results. Figure 4(b) clearly shows the C-TiO₂ nanocrystal present in the form of rectangular slab, and rod. This is also similar to images obtained from SEM analysis. The selected area electron diffraction pattern is shown in Figure 3(c) and the pattern indicates the discernible Debye Scherer rings of (101) (211) and (116) diffractions which are characteristic peaks of the anatase phase of TiO₂.

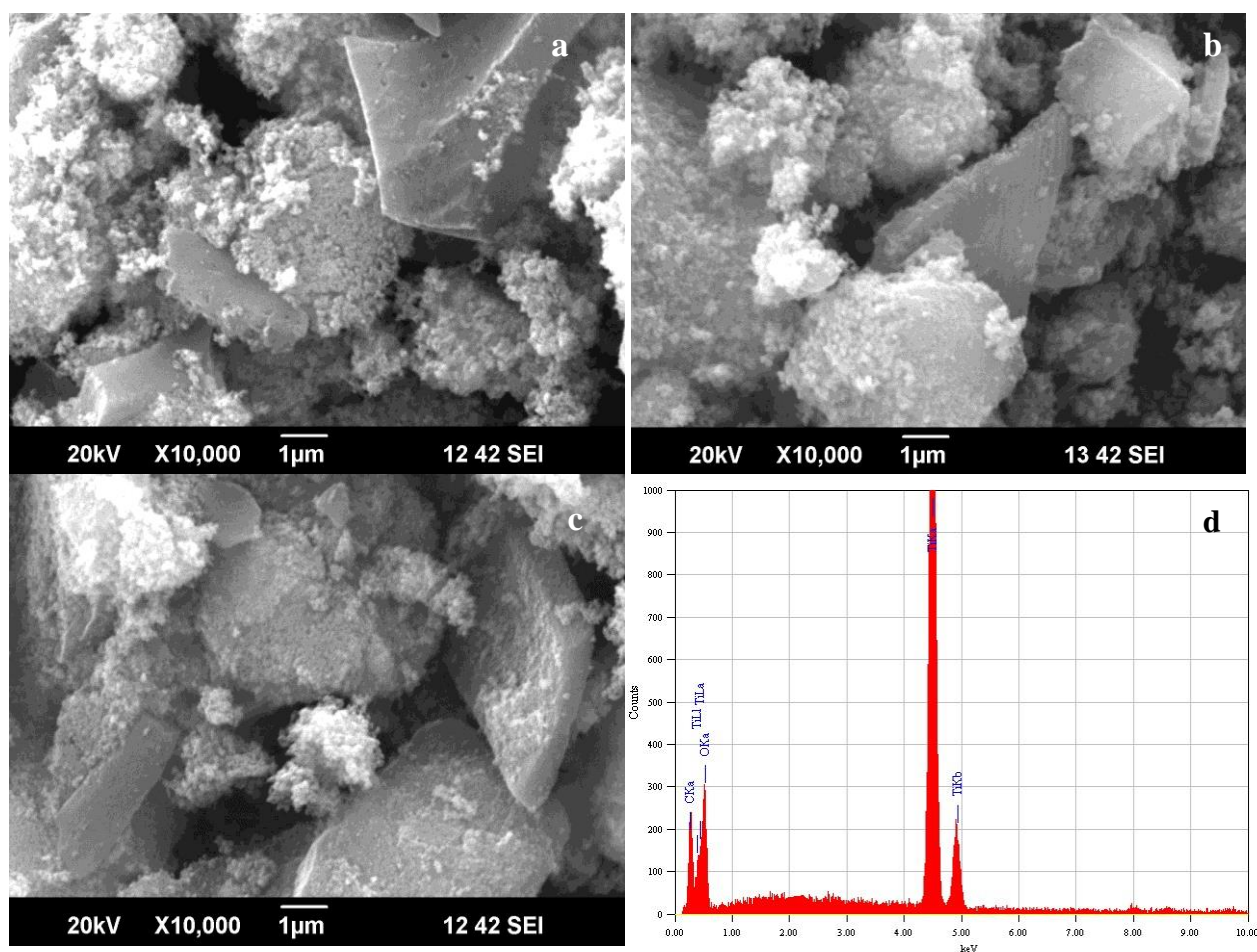


Fig 2. SEM images of C-TiO₂ nanocrystals prepared using (a) pH=2.6 (b) pH=7 and pH=10.6 and (d) EDXA of C-TiO₂ nanocrystals prepared using pH=10.6

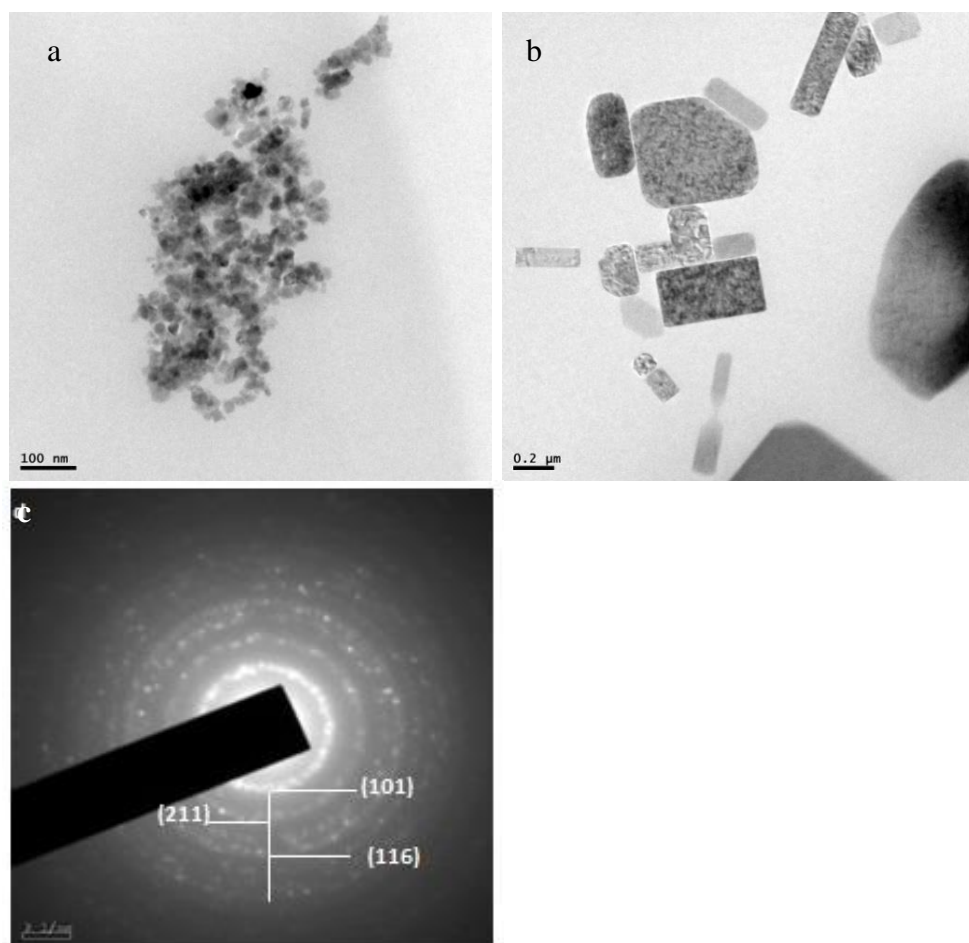


Fig. 3. TEM and SAED pattern of C-TiO₂ nanocrystals prepared at pH=10.6.

The UV-Vis absorption spectra of C-TiO₂ nanocrystals are shown in Figure 4. The absorption edge is found to vary for different pH value which is due to the variation of particle size with pH values and this result is also similar to the results reported by Yurdakal et al [24]. The photo catalytic activity mainly depends on the rate of e-h recombination, if the e-h recombination rate is high, the photo catalytic activity gets decreases [25] and hence it is necessary to improve the light absorption in the visible range. As the carbon doped TiO₂ nanocrystalline thin film absorbs more light it can be assumed that the carbon doped TiO₂ nanocrystalline thin film may have higher visible photo catalytic activity [26]. The red shift of absorption edge for the TiO₂ nanocrystals prepared at higher pH values corresponds to the band gap narrowing and it could be attributed to the carbon doping [27].

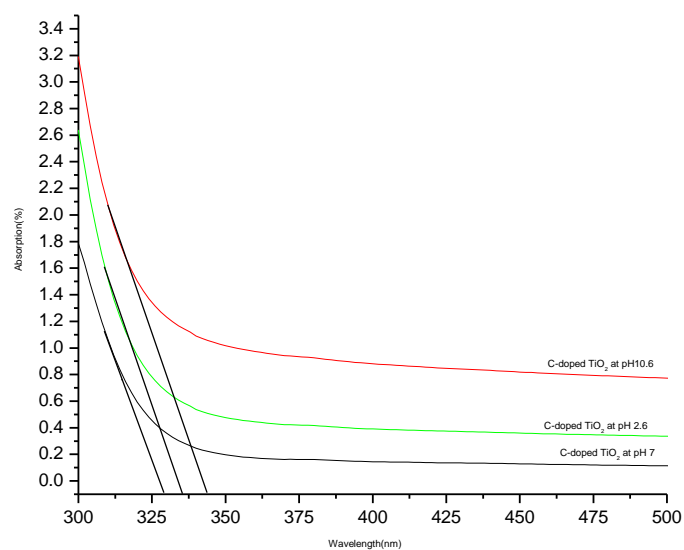


Fig. 4. UV-Vis absorption spectra of C-TiO₂ nanocrystals prepared at different pH values

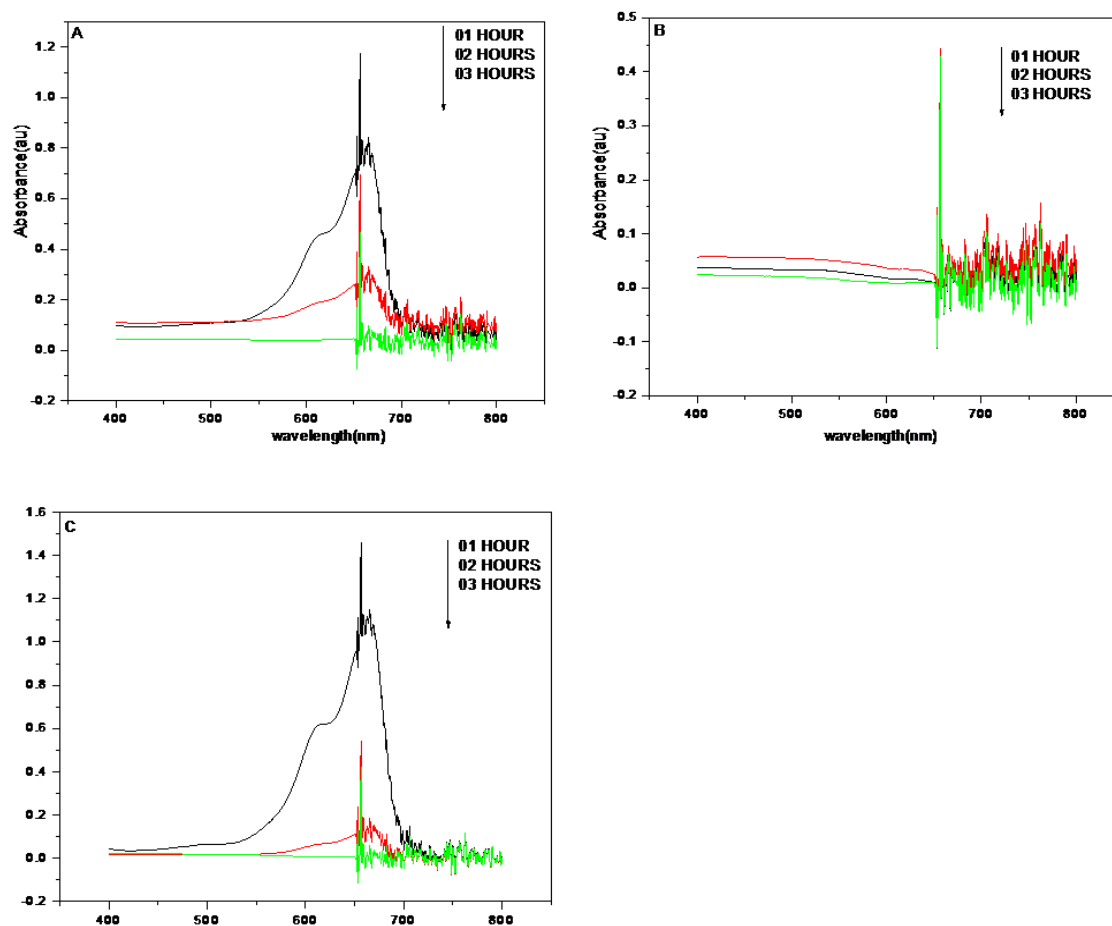


Fig. 5. The time dependent UV-Vis absorption spectra of methylene blue subjected to C-TiO₂ nanocrystalline thin films synthesized using different pH values a) 7, b) 2.6 and c) 10.6

Figures 5 (a, b and c) show the typical time dependent UV–Vis spectra of methylene blue dye during photo irradiation with C-TiO₂ thin films. The rate of decolourization was recorded with respect to the change in the intensity of absorption peak in visible region. The prominent peak is observed at λ_{\max} of 656.50 nm which decreased gradually with increase of irradiation time from 1 hour to 3 hours, the percentage degradation (% D) was calculated using the following equation.

$$\text{Percentage of degradation (\%D)} = (A_0 - A_t / A_0) * 100$$

Where A_0 = absorbance at $t = 0$ minute

A_t = absorbance at t minute

For the degradation experiments, fixed amount (10ppm) of methylene blue dye was taken in a beaker and the nanocrystalline carbon doped TiO₂ thin film was suspended inside the beaker. The beaker was subjected to irradiation under UV light (8W Philips bulb TUV-08) kept at a distance of 15 cm for fixed interval of time. Figure 6 (a, b and c) shows the effect of irradiation time of the catalyst on the decolourization of methylene blue. It can be observed that the initial slopes of the curves representing rate of decolourization, increases greatly with increasing irradiation time. The catalyst dosage also decided the photo catalytic destruction of other organic pollutants [28]. This can be explained on the basis of catalyst loading which is found to be dependent on initial solute concentration because with the increase in catalyst dosage, total active surface area increases. Hence availability of more active sites on catalyst surface increases [29].

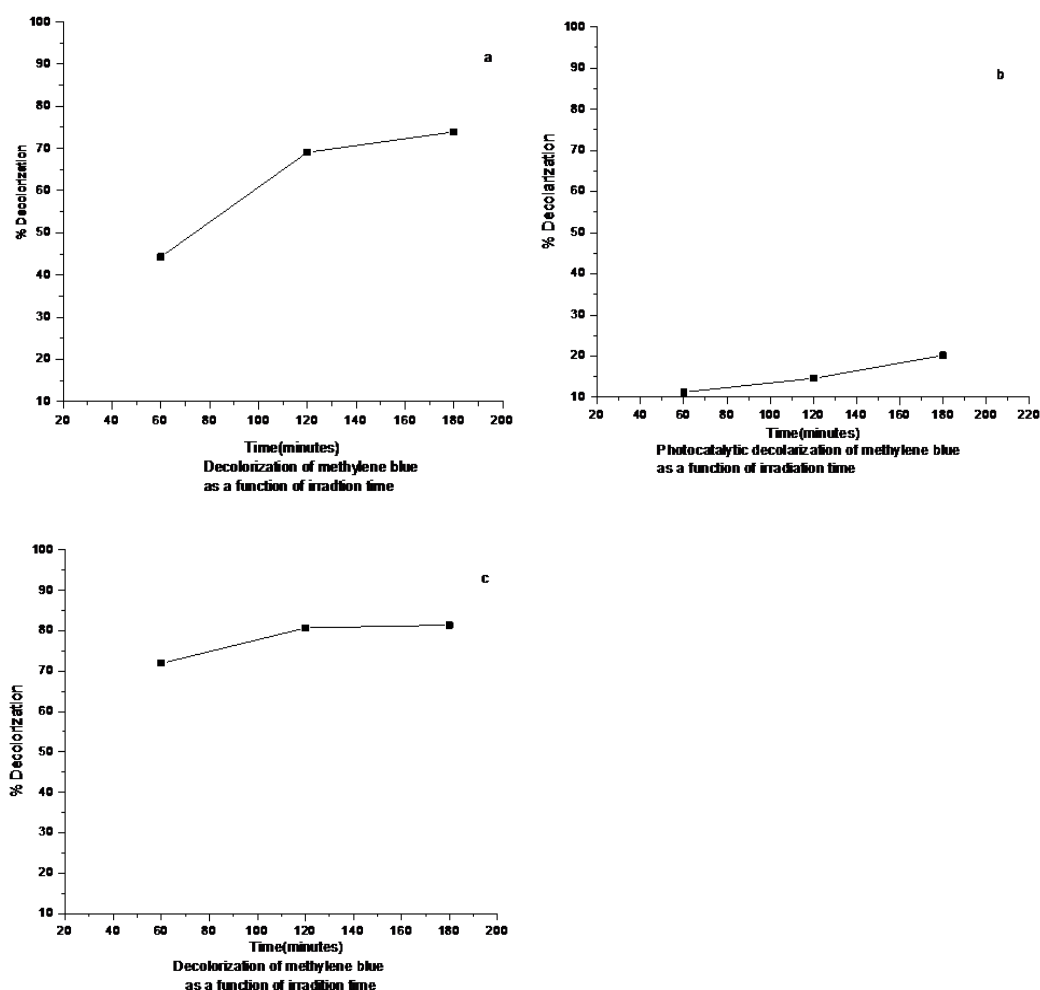


Fig. 6. Photocatalytic decolorization of methylene blue as a function of irradiation time by the C-TiO₂ nanocrystalline thin films synthesized using different pH values a) 7, b) 2.6 and c) 10.6

The degradation of the methylene blue is studied by using UV spectrophotometer of type UV-1800 series. It is observed from the Figure 5 that the maximum absorbance wavelength corresponds to methylene blue dye is 656.50 nm. The intensity of the peak corresponding to the maximum wavelength decreases as time increases i.e., the degradation of methylene blue is in proportion with time. The degradation of methylene blue by the nanocrystalline carbon doped TiO₂ thin film synthesized using pH=2.6 is 20.16%. This poor degradation of methylene blue by the nanocrystalline carbon doped TiO₂ thin film is due to positive surface charge on the TiO₂ nano crystalline surface. The positive charge on the TiO₂ surface does not pay attention to attract the methylene blue molecule since it is a cationic dye [30]. The degradation of methylene blue by the nanocrystalline carbon doped TiO₂ thin film using pH=7 is 73.91%. The degradation of methylene blue by the nanocrystalline carbon doped TiO₂ thin film synthesized using pH=10.6 is 81.45%. This may be due to the negative surface charge on the TiO₂ nano crystalline surface these charge readily attract the methylene blue molecule and degrade it.

4. Conclusion

Nanocrystalline carbon doped TiO₂ Thin films have been successfully prepared by loading carbon on TiO₂ nanocrystalline material synthesized using different pH conditions Results indicate that the light absorption extends to the visible region for the nanocrystalline carbon doped TiO₂ thin film synthesized using pH=10.6. The doping of carbon with nano crystalline TiO₂ material enhances the photocatalytic activity. In our work it is found that the nanocrystalline carbon doped TiO₂ thin film synthesized using pH=10.6 has the highest photocatalytic activity under UV radiation. The negative surface charge on the nanocrystalline TiO₂ material synthesized at higher pH (pH=10.6), and the interaction between the carbon and TiO₂ nanocrystalline material may be responsible for the high photocatalytic activity.

References

- [1] Xiaoxia Lin, Fei Rong, Degang Fu, Chunwei Yuan, Powder technology, **219**, 173 (2012).
- [2] Ming Shen, Zunyi Wu, Hui Huang, Yukou Du, Zhigang Zou, Ping Yang, Materials Letters, **60**, 693 (2006).
- [3] Sang-Hyeun Lee, Misook Kang, Sung M. Cho, Gui Young Han, Byung-Woo Kim, Ki June Yoon, Chan-Hwa Chung, Journal of Photochemistry and Photobiology A: Chemistry, **146**, 121 (2001).
- [4] Xin Li, Haoliang Liu, Deliang Luo, Jingtian Li, Ying Huang, Huiling Li, Yuehua Xu, Li Zhu, Yueping, Chemical Engineering Journal, **180**, 151 (2012).
- [5] W. Macyk, H. Kisch, Chem. Eur. J. **7**, 1862 (2001).
- [6] Yuanzhi Li, Doo-Sun Hwang, Nam Hee Lee, Sun-Jae Kim, Chemical Physics Letters, **404**, 25 (2005).
- [7] S. Klosek, D. Raftery, J. Phys. Chem. B. **105**, 2815 (2001).
- [8] Wenjie Ren, Zhihui Ai, Falong Jia, Lizhi Zhang, Xiaoxing Fan, Zhigang Zou, Applied Catalysis B: Environmental. **69**, 138 (2007).
- [9] R. Asashi, T. Morikawa, T. Ohwaki, K. Aoki, Y. Taga, Science, **293**, 269 (2001).
- [10] C. Burda, Y.B. Lou, X.B. Chen, A.C. Samia, J. Stout, J.L. Gole, Nano Lett. **3**, 1049 (2003).
- [11] H. Irie, Y. Watanabe, K. Hashimoto, Chem. Lett. **32**, 772 (2003).
- [12] S. Sakthivel, H. Kisch, Angew. Chem. Int. Ed. **42**, 4908 (2003).
- [13] T. Umabayashi, T. Yamaki, H. Itoh, K. Asai, Appl. Phys. Lett. **81**, 454 (2002).
- [14] HaoWang and James P Lewis, J. Phys. Condens. Matter. **17**, L209 (2005).
- [15] Yeon Seok Kim, Le Thuy Linh, Eun Seok Park, Sungmin Chin, Gwi-Nam Bae, Jongsoo Jung, Powder technology, **215-216**, 195 (2012).
- [16] Zs. Pap, L. Baia, K. Mogyorosi, A. Dombi, A. Oszko, V. Danciu, Catalysis Communications,

- 17**, 1 (2012).
- [17] Hyeok Choi, Elais Stathato, Dionysios D. Dionysiou, *Applied catalysis B: Environmental*, **63**, 60 (2006).
- [18] Gang Yu, Zhongying Chen, Zulin Xhang, *Catalysis Today*, **90**, 305 (2004).
- [19] T.S. Senthil, N. Muthukumarasamy, S. Agilan, M. Thambidurai, R. Balasundaraprabhu, *Materials Science and Engineering B* **174**, 102 (2010).
- [20] A. Testino, I.R. Bellobono, V. Buscaglia, C. Canevali, M. D'Arienzo, S. Polizzi, R. Scotti, F. Morazzoni, *J. Amer. Chem. Soc.* **129**, 3564 (2007).
- [21] X. Chen, S.S. Mao, *Chem. Rev.* **107**, 2891 (2007).
- [22] J. Chae, D.Y. Kim, S. Kim, M. Kang, *J. Ind. Eng. Chem.* **16**, 906 (2010).
- [23] Mingyang Xing, Jinlong Zhan, Feng Chen, *Applied Catalysis B: Environmental*, **89**, 563 (2009).
- [24] Yurdakal Sedat, Vittorio Loddo, Bernardi Bayarri Ferrer, Giovanni Palmisano, Vincenzo Augugliaro, Jaime Gimenez Farreras, and Leonardo Palmisano, *Ind. Eng. Chem. Res.*, **46**, 7620 (2007).
- [25] Hui Zhang, Hong Zhu, *Applied Surface Science*, **258**, 10034 (2012).
- [26] Xiaoxia Lin, Fei Rong, Xiang Ji, Degang Fu, *Microporous and Mesoporous Materials*, **142**, 276 (2011).
- [27] Penghua Wang, Pow-Seng Yap, Teik-Thye Lim, *Applied Catalysis A: General*, **399**, 252 (2011).
- [28] A. Akyol, H. C. Yatmaz, M. Bayramoglu, *Appl. Catal. B Environ.* **54**, 19 (2004).
- [29] M. S. T. Gonclaves, A. M. F. Oliveira-Campos, E. M. M. S. Pinto, P. M. S. Plasencia, M. J.R. P Queiroz, **39**(5), 781 (1999).
- [30] Chin Mei Ling Abdul Rahman, Mohamed, Subhash Bhatia, *Chemosphere*, **57**, 547 (2004).